

# Solar Second Harmonic Plasma Emission and the Head-on Approximation

A. J. Willes, P. A. Robinson and D. B. Melrose

Department of Theoretical Physics and Research Centre  
for Theoretical Astrophysics, School of Physics,  
University of Sydney, NSW 2006, Australia  
a.willes@physics.usyd.edu.au

Received 1994 August 19, accepted 1995 January 31

**Abstract:** The coalescence of two Langmuir waves,  $L$  and  $L'$ , produces emission at twice the plasma frequency in type II and type III solar radio bursts. The analysis of the coalescence process is usually simplified by assuming the head-on approximation, where the wavevectors of the coalescing waves satisfy  $\mathbf{k}_{L'} \approx -\mathbf{k}_L$ , corresponding to the two Langmuir waves meeting head on. However, this is not always a valid approximation, particularly when the peak of the Langmuir spectrum lies at small wavenumbers, for narrow band spectra, and for spectra with broad angular ranges. Realistic Langmuir wave spectra are used to investigate the effects of relaxing the head-on approximation.

**Keywords:** radiation mechanisms: nonthermal — Sun: radio radiation — Sun: corona

## 1. Introduction

Simultaneous plasma emission at the fundamental and second harmonic of the plasma frequency is a common phenomenon in type II and type III solar radio bursts. In both cases, nonlinear wave-wave interactions are the favoured explanation, first proposed in this context by Ginzburg and Zheleznyakov (1958), and extended by Melrose (1970a,b, 1980). The parent waves in these interactions are Langmuir waves, driven by unstable electron beams. In type II bursts, which are associated with magnetohydrodynamic shock waves in the solar corona, the Langmuir waves are assumed to be generated by streaming electrons accelerated by the shock, or shock-related phenomena (Ginzburg & Zheleznyakov 1958; Smith 1972). This theory satisfactorily explains the ‘herringbone’ structure but not the ‘backbone’ emission in type II bursts (Nelson & Melrose 1985). In type III bursts, the Langmuir waves are driven by unstable electron beams travelling out from the solar corona, escaping from the energy release region of a flare. The spectrum of primary Langmuir waves  $L$  is concentrated about the wavevector  $k_L$ , parallel to the direction of the beam. The wavenumber  $k_L$  is determined by the beam velocity of the streaming electrons, and the width of the spectrum is determined by the width of the electron beam. The first nonlinear three-wave process of relevance is electrostatic backscatter decay, where the primary Langmuir waves decay into product Langmuir waves  $L'$  and ion sound waves  $S$  via the process  $L \rightarrow L' + S$ . The spectrum

of backscattered Langmuir waves is distributed about the parallel wavevector  $\mathbf{k}_{L'}$ , antiparallel to the direction of the beam, with magnitude  $k_{L'} = -(k_L - k_0)$ , with  $k_0 \ll k_L$  determined by the ion sound speed (Cairns 1986, 1987a; Robinson, Willes & Cairns 1993). The wavenumber difference satisfies  $k_0 = 2(\gamma m_e/m_i)^{1/2} k_D/3$ , where  $\gamma$  is the ratio of specific heats with  $\gamma = 1 + 3T_i/T_e$ , and  $k_D$  is the Debye wavenumber. Typical Langmuir spectra for the primary and backscattered Langmuir waves are shown in Figure 1. The forms of these spectra are determined from theoretical and numerical work (Robinson, Newman & Rubenchik 1993; Robinson et al. 1992; Robinson & Newman 1989). Repeated backscattered decays are also possible (Robinson et al. 1992; Robinson & Newman 1989), where a cascade of such decays leads to a condensate of Langmuir waves at low wavenumbers. The number of

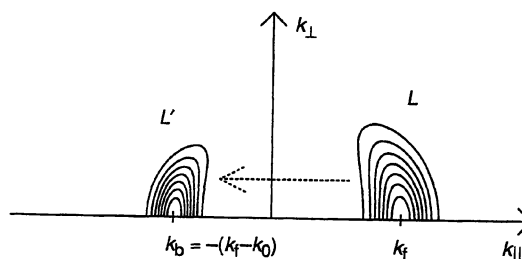


**Figure 1**—Langmuir waves are generated in the primary spectrum  $L$  by an unstable beam of electrons. These undergo the process of backscatter decay to produce Langmuir waves  $L'$  (at lower wavenumbers) propagating in the opposite direction.

backscatter decays is limited by the kinematics. The second relevant three-wave process is fundamental emission, where a Langmuir wave decays into a transverse electromagnetic wave  $T$  at the plasma frequency  $\omega_p$  and another ion sound wave  $S'$  via the process  $L \rightarrow T + S'$ . The transverse electromagnetic waves  $T$  are observed as fundamental emission. The third process is second harmonic emission (at twice the plasma frequency) produced through coalescence between a primary and a backscattered Langmuir wave:  $L + L' \rightarrow T'$ . We consider this process in detail in this paper.

Most previous theoretical analyses of the process of Langmuir wave coalescence have assumed the head-on approximation (Smith 1970; Melrose 1980; Cairns 1986, 1987b). This requires that the wavenumber of the Langmuir waves far exceeds that of the product second harmonic transverse waves, i.e.  $k_L \gg k_T$ . Through momentum conservation for the process  $L + L' \rightarrow T$ , the wavevectors satisfy  $\mathbf{k}_L + \mathbf{k}_{L'} = \mathbf{k}_T$ . This wavevector addition is illustrated in Figure 2 when the head-on condition  $k_L \gg k_T$  is satisfied. It is clear from Figure 2 that  $\mathbf{k}_L \approx \mathbf{k}_{L'}$ , i.e. the two coalescing Langmuir waves meet head-on. The effect of relaxing the head-on approximation has been investigated for isotropic Langmuir spectra, assuming a power-law form for the spectra (Melrose & Stenhouse 1979). In this case, the head-on approximation overestimates the rate of production of second harmonic waves when the condition  $k_L \gg k_T$  is not satisfied. The aim of this paper is to investigate the relaxation of the head-on approximation for the (anisotropic) primary and backscattered Langmuir spectra mentioned above.

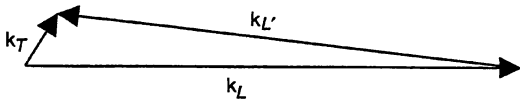


**Figure 2**—Wavevector conservation for the coalescence process  $L(\mathbf{k}_L) + L'(\mathbf{k}_{L'}) \rightarrow T(\mathbf{k}_T)$ , where  $\mathbf{k}_L + \mathbf{k}_{L'} = \mathbf{k}_T$ . The condition for the head-on approximation,  $k_L \gg k_T$ , implies  $\mathbf{k}_L \approx -\mathbf{k}_{L'}$ .

## 2. Exact Treatment

The rate of production of transverse waves  $T$  through the process  $L + L' \rightarrow T$  is given by the relation (Melrose & Stenhouse 1979)

$$\frac{\partial T^T}{\partial t}(\mathbf{k}_T) = \frac{2}{\hbar\omega_p} \int \frac{d^3\mathbf{k}_1}{(2\pi)^3} \int \frac{d^3\mathbf{k}_2}{(2\pi)^3} \times u_{T12}(\mathbf{k}_T, \mathbf{k}_1, \mathbf{k}_2) T^L(\mathbf{k}_1) T^L(\mathbf{k}_2), \quad (1)$$

with

$$u_{T12}(\mathbf{k}_T, \mathbf{k}_1, \mathbf{k}_2) = \frac{e^2 \hbar}{32 \epsilon_0 m_e^2 \omega_p} \frac{(k_1^2 - k_2^2)^2 |\hat{\mathbf{k}}_1 \times \hat{\mathbf{k}}_2|^2}{k_T^2} \times (2\pi)^4 \delta^3(\mathbf{k}_T - \mathbf{k}_1 - \mathbf{k}_2) \times \delta(\omega_T(\mathbf{k}_T) - \omega_L(\mathbf{k}_1) - \omega_L(\mathbf{k}_2)), \quad (2)$$

where the transverse waves are described in terms of their brightness temperature  $T^T(\mathbf{k}_T)$  and the Langmuir waves in terms of their effective temperature  $T^L(\mathbf{k}_{1,2})$ , and  $\hat{\mathbf{k}} = \mathbf{k}/k$ . The subscripts 1 and 2 refer to the two coalescing Langmuir waves. The delta function in frequency expresses conservation of energy of the coalescing quanta, while that in wavevectors ensures conservation of momentum. The six-dimensional integral (1) can be reduced to two dimensions by use of the four delta functions, and can then be reduced to one dimension by choosing an appropriate form for the Langmuir spectra  $T_L(\mathbf{k})$ . This one dimensional integral may be evaluated numerically.

There are kinematic restrictions on the coalescence process due to frequency and wavevector conservation. The thermal electron temperature must exceed  $T_e = 4.8 \times 10^5$  K for the process to proceed (Melrose 1982), although lower temperatures are allowable for finite widths of the Langmuir spectra (Cairns 1986, 1987b). Kinematic restrictions also imply a maximum thermal electron temperature,  $T_e = 1.0 \times 10^9$  K above which the process cannot occur. Restrictive kinematic effects occur for temperatures above  $T_e = 5.3 \times 10^8$  K. Typical values of the thermal electron temperature are  $T_e = (1.5 - 2.0) \times 10^5$  K (Lin et al. 1981) for interplanetary type III solar radio bursts and  $T_e = (1.5 - 2.0) \times 10^6$  K for coronal type III bursts.

In our numerical analysis, we assume a Gaussian form for the Langmuir spectra,

$$T^L(\mathbf{k}) = \zeta T_f \exp \left[ \frac{-(k_{\parallel} - k_f)^2 - k_{\perp}^2}{K^2} \right] + (1 - \zeta) T_b \exp \left[ \frac{-(k_{\parallel} - k_b)^2 - k_{\perp}^2}{J^2} \right], \quad (3)$$

where  $0 \leq \zeta \leq 1$  is the fractional energy in the primary (forward) spectrum,  $k_f$  is the wavenumber at which the primary Langmuir spectrum peaks,  $K$  is the width of the primary spectrum,  $k_b$  is the wavenumber at which the backscattered Langmuir spectrum peaks,  $J$  is the width of the backscattered

spectrum, and  $T_f$  and  $T_b$  are normalisation factors. The spectra (3) must satisfy the normalisation

$$\int \frac{d^3\mathbf{k}}{(2\pi)^3} T^L(\mathbf{k}) = U, \quad (4)$$

where  $U$  is the energy density in the Langmuir waves.

### 3. The Head-on Approximation

In the three-wave process  $L(\omega_L, \mathbf{k}_L) + L'(\omega_{L'}, \mathbf{k}_{L'}) \rightarrow T(\omega_T, \mathbf{k}_T)$ , the following kinematic conditions must be satisfied, corresponding to conservation of energy and momentum,

$$\omega_L + \omega_{L'} = \omega_T, \quad (5)$$

$$\mathbf{k}_L + \mathbf{k}_{L'} = \mathbf{k}_T. \quad (6)$$

The head-on approximation corresponds to  $\mathbf{k}_L, \mathbf{k}_{L'} \ll \mathbf{k}_T$ , whence (6) implies  $\mathbf{k}_{L'} \approx -\mathbf{k}_L$ , i.e. the two coalescing Langmuir waves meet head-on. The transverse waves satisfy the dispersion relation

$$\omega_T(k_T) = (\omega_p^2 + k_T^2 c^2)^{\frac{1}{2}}. \quad (7)$$

Hence, for  $\omega_T = 2\omega_p$  (second harmonic transverse waves), the relation (7) implies

$$k_T \approx \frac{\sqrt{3}\omega_p}{c}. \quad (8)$$

For symmetrically placed ( $k_b = -k_f$ ) Gaussian Langmuir spectra with equal widths ( $J = K$ ), the expression (1) reduces to

$$\frac{\partial T^T}{\partial t} = \frac{T_f^2 e^2 \omega_p K^2 \sin^2 \chi \cos^2 \chi}{2^{\frac{1}{2}} 256 \pi \epsilon_0 m_e^2 V_e^2 c^2 k_f}, \quad (9)$$

in the head-on approximation, and using (8). The angle  $\chi$  is that between the  $k_{\parallel}$  axis (along the direction of the electron beam) and the wavevector  $\mathbf{k}_T$ , and  $V_e$  is the thermal electron speed. Hence, in the head-on approximation, the maximum rate of production of transverse electromagnetic waves occurs at  $\chi = 45^\circ, 135^\circ$  to the beam direction. For these angles the maximum rate of production is given by

$$\left. \frac{\partial T^T}{\partial t} \right|_{\max} = \frac{T_f^2 e^2 \omega_p K^2}{2^{\frac{1}{2}} 1024 \pi \epsilon_0 m_e^2 V_e^2 c^2 k_f}. \quad (10)$$

The exact solution, in the form of a one-dimensional integral, satisfies

$$\begin{aligned} \frac{\partial T^T}{\partial t}(k_T, \chi) &= f(T_f, T_f, k_f, k_f, K, K, \zeta, \zeta) \\ &+ f(T_f, T_b, k_f, k_b, K, J, \zeta, 1 - \zeta) \\ &+ f(T_b, T_f, k_b, k_f, J, K, 1 - \zeta, \zeta) \\ &+ f(T_b, T_b, k_b, k_b, J, J, 1 - \zeta, 1 - \zeta), \end{aligned} \quad (11)$$

where

$$\begin{aligned} f(T_f, T_b, k_f, k_b, K, J, \zeta, 1 - \zeta) &= \frac{\zeta(1 - \zeta) T_f T_b e^2}{96 \pi \epsilon_0 \omega_p m_e^2 V_e^2} \\ &\times \int_{-1}^1 dx \frac{k_1^2 (1 - x^2) (2k_1^2 - k_*^2)^2}{(k_*^2 - k_1^2) \sqrt{k_T^2 x^2 + 2k_*^2 - 2k_T^2}} \\ &\times \exp \left[ - \frac{k_1^2 - k_f^2 + 2k_1 k_f \cos \chi x}{K^2} \right. \\ &\left. + \frac{-k_1^2 - k_b^2 - 2k_1 k_b \cos \chi x - k_T^2 + 2k_T k_1 x + 2k_T k_b \cos \chi}{J^2} \right] \\ &\times I_0 \left[ 2k_1 \left( \frac{k_f}{K^2} - \frac{k_b}{J^2} \right) \sqrt{1 - x^2} \sin \chi \right], \end{aligned} \quad (12)$$

where

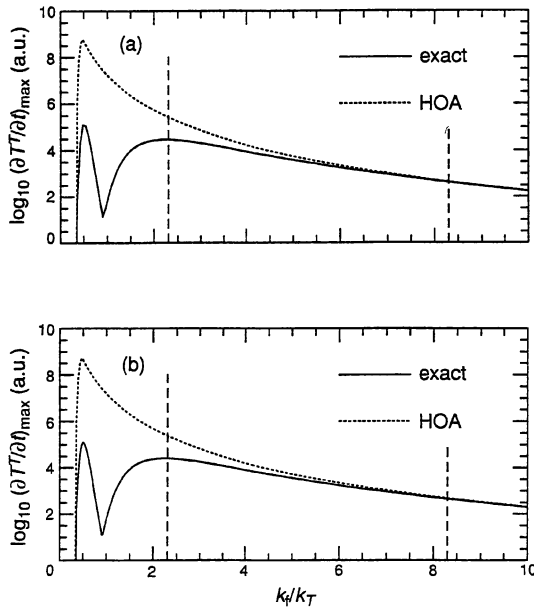
$$k_1 = \frac{1}{2} \left\{ k_T x + \sqrt{k_T^2 x^2 + 4\omega_p(\omega_T(k_T) - 2\omega_p)/(3V_e^2) - 2k_T^2} \right\}. \quad (13)$$

The maximum rate of production is determined by maximising this expression over  $k_T$  and  $\chi$ .

### 4. Results

We consider the variation of the maximum rate of production of second harmonic electromagnetic waves as a function of  $k_f$ , the peak wavenumber of the primary Langmuir spectrum. The parameters are chosen as typical observed values for interplanetary and coronal type III bursts. The speed of the electron beams is usually quoted to be in the range  $v_b = (0.1-0.5)c$  with faster beam speeds in the corona than in the interplanetary medium. However more recent measurements have determined that the speeds are in the range  $v_b = (0.07-0.25)c$  (average  $0.14c$ ) with no overall change in the beam speed with distance from the Sun (Dulk et al. 1987). This corresponds to the primary Langmuir spectra peaking at wavenumbers in the range  $k_f = (2.3-8.3)k_T$ , using  $k_f = \omega_p/v_b$ . Lower wavenumbers than these can be obtained through repeated backscatter decays, or for the case of type IIIId bursts (Poquérousse 1994) which have relativistic electron beam speeds. Typical beam widths for type III bursts are in the range  $\Delta v_b/v_b = 0.1-0.3$  (Lin et al. 1981), implying spectral

widths  $K = (0.1-0.3)k_f$ . We choose  $K = 0.2k_f$  for the following results. For interplanetary type III bursts, we assume typical values for the plasma frequency  $\omega_p = 1.5 \times 10^5 \text{ s}^{-1}$  and the thermal electron velocity  $V_e = 1.5 \times 10^6 \text{ m s}^{-1}$ . Similarly, for coronal type III bursts,  $\omega_p = 1.5 \times 10^8 \text{ s}^{-1}$  and  $V_e = 5.0 \times 10^6 \text{ m s}^{-1}$ .



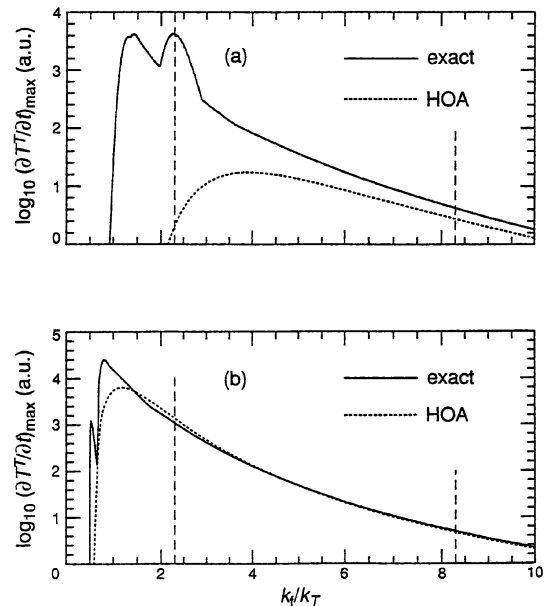
**Figure 3**—A plot of  $\log_{10}(\partial T/\partial t)_{\max}$ , the maximum rate of production (arbitrary units) of second harmonic transverse electromagnetic waves as a function of  $k_f$ , the peak of the primary Langmuir spectrum in wavenumber space, for (a)  $\omega_p = 1.5 \times 10^5 \text{ s}^{-1}$ ,  $V_e = 1.5 \times 10^6 \text{ m s}^{-1}$  and (b)  $\omega_p = 1.5 \times 10^8 \text{ s}^{-1}$ ,  $V_e = 5.0 \times 10^6 \text{ m s}^{-1}$ . The exact solution is marked with a solid curve, the head-on approximation with a dashed curve. The range of wavenumbers relevant to observed solar parameters for type III solar radio bursts lies between the vertical dashed lines.

Figure 3 shows the maximum rate of production of second harmonic transverse electromagnetic waves as a function of  $k_f$ , the peak wavenumber of the primary Langmuir spectrum for symmetric Langmuir spectra ( $k_b = -k_f$ ). Figure 3a is for the interplanetary burst parameters, and Figure 3b for the coronal burst parameters. Both the exact solution, obtained through numerical integration of (1) for the Langmuir spectra (3) (see Section 2), and the head-on solution (10) are shown. The head-on approximation clearly overestimates this rate for Langmuir spectra at low wavenumbers. For the range of wavenumbers consistent with the observed electron beam velocities in typical type III bursts (marked in Figure 3), the head-on approximation overestimates the exact value by  $\lesssim 10$  times. For electron beam widths at the lower end of the observed range ( $K = 0.1k_f$ ), this overestimate ranges between 10 and 100 times. For wider beam widths (corresponding to wider Langmuir spectra) the head-on approximation improves, i.e.

it is valid to lower wavenumbers. The cutoff, at  $k_f \approx k_T$ , occurs because the pair of oppositely directed coalescing Langmuir waves do not satisfy the condition  $|k_L - k_{L'}| \approx k_T$  for momentum conservation, with  $k_f \lesssim k_T$ .

In Figure 4 the wavenumber offset in the backscattered Langmuir spectrum ( $k_b = k_0 - k_f$ ) is included, where the ratio of specific heats  $\gamma$  is assumed to be unity. For the interplanetary burst parameters (Figure 4a) the head-on approximation underestimates the exact solution, particularly at the lower wavenumbers. For coronal parameters (Figure 4b) the agreement is good. For the coronal burst parameters, the offset parameter  $k_0$  is smaller than for the interplanetary burst parameters. Hence the agreement between the head-on approximation and the exact solution for the coronal parameters with the offset ( $k_0 = 0.6k_T$ ) lies between the overestimate of the symmetric case ( $k_0 = 0.0$ ) and the underestimate of the offset interplanetary case ( $k_0 = 1.9k_T$ ). We conclude from both the symmetric and offset cases that the head-on approximation is unreliable at low wavenumbers, overestimating the rate for symmetric Langmuir spectra and tending to underestimate the rate for the offset backscatter spectra.

For large values of  $k_f$ , where the condition ( $k_L \gg k_T$ ) for the head-on approximation (see Figure 2) is satisfied, the exact and head-on cases agree well. This is where a Langmuir wave from the primary spectrum (centred at  $k_{\parallel} = k_f$ ) coalesces with a Langmuir wave from the backscattered spectrum



**Figure 4**—Similar to Figure 3 but with the offset included in the backscattered Langmuir spectrum ( $k_b = k_0 - k_f$ ): (a)  $k_0 = 1.9k_T$  and (b)  $k_0 = 0.6k_T$ .

(centred at  $k_{\parallel} = -k_f$ ) to produce the second harmonic transverse wave. Here, the exact case also predicts that the maximum rate of emission occurs at angles  $\chi = 45^\circ, 135^\circ$  to the beam direction, as in the head-on approximation. At very low wavenumbers,  $k_f \approx \frac{1}{2}k_T$ , there is an additional peak in the exact solution. This is due to two Langmuir waves travelling in the same direction with  $k_L \approx \frac{1}{2}k_T$  coalescing to produce a transverse wave with wavenumber  $k_T$ . In the offset case (Figure 4) the two peaks correspond to  $k_b = \pm \frac{1}{2}k_T$ . The wavevector addition for this process is illustrated in Figure 5, in analogy to Figure 2 for the head-on approximation. In this case the two coalescing Langmuir waves come from the same spectrum, and the maximum rate of production of second harmonic waves occurs at angles  $\chi = 0^\circ$  for the primary spectrum and  $\chi = 180^\circ$  for the backscattered spectrum. This effect is not predicted by the head-on approximation, and is particularly important when a cascade of backscatter decays creates a condensate of Langmuir waves at low wavenumbers.

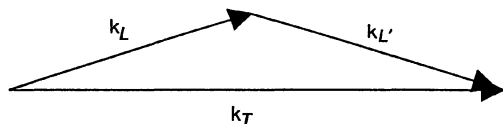


Figure 5—Langmuir wave coalescence at low wavenumbers. Two Langmuir waves with wavenumbers  $k_L, k_{L'} \approx \frac{1}{2}k_T$  coalesce to produce a transverse wave, with wavenumber  $k_T$ .

## 5. Conclusions

The process of two-Langmuir-wave coalescence to produce second harmonic transverse electromagnetic waves is the accepted mechanism for second harmonic radio emission in solar radio bursts. Usually, it is assumed that the Langmuir waves are generated at sufficiently high wavenumbers that the condition  $k_L \gg k_T$  for the head-on approximation is satisfied. However, for typical solar type III burst parameters, which imply  $k_f = (2.3-8.3)k_T$ , and with backscatter cascades which create Langmuir waves at progressively lower wavenumbers, this condition is not satisfied.

In this paper, model spectra for the primary and backscattered Langmuir waves are used in an exact numerical solution for the rate of production of second harmonic waves. This is compared to the analytic result derived assuming the head-on approximation, i.e. where the two coalescing Langmuir waves approach from opposite directions. For large  $k_f$  (where the Langmuir spectra peak at

high wavenumbers), the exact and head-on solutions agree well, both predicting the same value for the rate of this process and the angle at which the maximum rate occurs ( $\chi = 45^\circ, 135^\circ$ ). However, at lower wavenumbers the head-on approximation becomes increasingly unreliable. Below the cutoff at low wavenumbers in the exact solution there is another feature corresponding to coalescence between two Langmuir waves from the same spectrum. In this case the angle at which the maximum rate occurs is  $\chi = 0^\circ, 180^\circ$ . This feature is completely missed by the head-on approximation. The validity of the head-on approximation also depends on the width of the Langmuir spectra: the narrower the spectral width, the poorer the approximation, as for spectral widths  $\lesssim k_T$  there are fewer pairs of oppositely directed Langmuir waves which satisfy  $|k_L - k_{L'}| \approx k_T$ .

For typical solar type III burst parameters (for both interplanetary and coronal bursts), the head-on approximation is not valid, particularly for narrow beam widths ( $\Delta v_b/v_b = 0.1$ ), and at the lower end of the wavenumber range.

## Acknowledgments

This work was supported by an Australian Postgraduate Award and the Australian Research Council.

- Cairns, I. H. 1986, PhD thesis, Univ. Sydney  
 Cairns, I. H. 1987a, *J. Plasma Phys.*, 38, 169  
 Cairns, I. H. 1987b, *J. Plasma Phys.*, 38, 179  
 Dulk, G. A., Steinberg, J. L., Hoang, S., & Goldman, M. V. 1987, *A&A*, 173, 366  
 Ginzburg, V. L., & Zheleznyakov, V. V. 1958, *Sov. Astron. AJ*, 2, 653  
 Lin, R. P., Potter, D. W., Gurnett, D. A., & Scarf, F. L. 1981, *ApJ*, 251, 364  
 Melrose, D. B. 1970a, *Aust. J. Phys.*, 23, 871  
 Melrose, D. B. 1970b, *Aust. J. Phys.*, 23, 885  
 Melrose, D. B. 1980, *Space Sci. Rev.*, 26, 3  
 Melrose, D. B. 1982, *Sol. Phys.*, 79, 173  
 Melrose, D. B., & Stenhouse, J. E. 1979, *A&A*, 73, 151  
 Nelson, G. J., & Melrose, D. B. 1985, in *Solar Radiophysics*, ed. D. J. McLean & N. R. Labrum (Cambridge Univ. Press)  
 Poquérousse, M. 1994, *A&A*, 286, 611  
 Robinson, P. A., & Newman, D. L. 1989, *Phys. Fluids B*, 1, 2319  
 Robinson, P. A., Newman, D. L., & Rubenchik, A. M. 1992, *Phys. Fluids B*, 4, 2509  
 Robinson, P. A., Willes, A. J., & Cairns, I. H. 1993, *ApJ*, 408, 720  
 Smith, D. F. 1970, *Adv. Astron. Astrophys.*, 7, 147  
 Smith, D. F. 1972, *ApJ*, 174, 643